DEEP HYBRID WAVELET NETWORK FOR ICE BOUNDARY DETECTION IN RADRA IMAGERY

Hamid Kamangir[1], Maryam Rahnemoonfar[1], Dugan Dobbs[1], John Paden[2], Geoffrey Fox[3]*

1: Texas A&M University-Corpus Christi, 2: The University of Kansas, 3: Indiana University

ABSTRACT

This paper proposes a deep convolutional neural network approach to detect Ice surface and bottom layers from radar imagery. Radar images are capable to penetrate the Ice surface and provide us with valuable information from the underlying layers of ice surface. In recent years, deep hierarchical learning techniques for object detection and segmentation greatly improved the performance of traditional techniques based on hand-crafted feature engineering. We designed a deep convolutional network to produce the images of surface and bottom ice boundary. Our network take advantage of undecimated wavelet transform to provide the higest level of information from radar images, as well as multilayer and multi-scale optimized architecture. In this work, radar images from 2009-2016 NASA Operation IceBridge Mission are used to train and test the network. Our network outperformed the state-of-the art accuracy.

Index Terms— Ice Boundary detection, Holistically nested edge detection, Wavelet transform, Radar, Deep learning

1. INTRODUCTION

Earth's rising temperature has a negative impact on subsurface mechanism of the earth polar regions which resulted in accelerated loss of ice from Greenland and Antarctica. Monitoring ice thickness and layers hidden beneath ice sheet is very important especially for predicting flood and sea level rise. Radar remote sensing images provide useful information about the hidden sub layers of ice over large area. The ice thickness can be estimated by calculating the distance between position of the ice surface and ice bottom layer in radar imagery.

Edge detection techniques have been studied most extensively and have a rich history in image processing and machine vision. Some traditional techniques, such as Sobel [1], Canny [2], zero-crossing [3], Boosted Edge Learning (BEL) [4], multiscale [5], and Structured Edges [6] frequently have been applied for detecting boundaries. In particular, several semi-automated and automated techniques have proposed for ice thickness boundary detection in radar images [7, 8, 9,

---

* Corresponding author.

10, 11]. These methods include filtering and thresholding techniques, statistical analysis of the signal [7], active contour [8], Level-set technique [10], and graphical models [11] to precisely detect the ice surface and the bottom boundary. These traditional computer vision techniques are based on hand crafted feature engineering and are not suitable for a large and complex dataset.

In recent years, Deep Learning (DL) algorithms have proved to be a new efficient technique to automatically learn features from data in a hierarchical manner. DL boundary detection techniques are mostly based on developing convolutional neural networks, such as N4-fields [12], Deep Contour [13], Deep Edge [14], CSCNN [15], and Holistically Nested Edge Detection (HED) [16] approach. Shen et al[13] proposed new deep learning technique for contour detection. They trained the network by partitioning contour patches into subclasses and fitting each subclass by different model parameters based on divide-and conquer strategy. Bertasius et al [14] exploited object related features as high-level cues for contour detection. To achieve this goal they designed a multi-scale network. Xie and Tu [16] proposed Holistically-Nested Edge Detection (HED). This technique is end-to-end edge detection technique, which is a type of Fully Convolutional Neural Network (FCN) but HED algorithm takes advantages of side outputs (multiple networks) which compensates the lack of deep supervision in FCN. Also, HED algorithm is a multiscale algorithm.

Motivated by fully convolutional network and deep supervision net in HED [16], we develop an end-to-end boundary detection network in combination with undecimated wavelet transformation technique for detecting ice layers in a large dataset. Figure 1 shows the architecture of our technique.

2. METHODOLOGY

Our network consist of two parts; The first part is for denoising the radar images. The second part is multi-scale neural network architecture to extract the edge maps. Radar images suffer from speckle noise, a signal dependent granular noise that degrades the quality of images [17]. The wavelet transformation is an efficient technique for reducing speckle noise in radar images. Wavelet transform provide the highest effective detail of image by decomposing it at different levels.
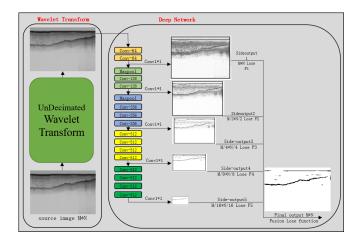
Fig. 1. Deep hybrid wavelet network architecture for boundary detection.

However, discrete wavelet transformation is translation variant and some important coefficients will be lost during transformation. Due to this fact, undecimated discrete wavelet transform (UDWT) [17, 18] is used at this research. The coefficients in the UDWT domain can be obtained by filtering the original signal by using of the following functions:

$$H_{eq,l}^j(z) = \prod_{m=0}^{j-1} H_0(z^{2^m}) \tag{1}$$

$$H_{eq,h}^j(z) = [\prod_{m=0}^{j-2} H_0(z^{2^m})].H_1(z^{2^j} - 1) \tag{2}$$

where l and h are the approximation (low level) and detail signals, respectively. Also, j denotes the level of decomposition.

In the first phase of our method following procedure is performed:

1. Smoothing the images: median filter and Savitzky-Golay filter [19] are used to smooth the images. The second one is used to smooth a noisy signal whose frequency span (without noise) is large. The performance of this filter is much better than standard averaging filters, because this filter preserves the relevant high frequency components of signal, and minimize the least square error by filtering a polynomial frame of noisy data.

2. Decomposing the image A into wavelet sub-bands $S(\epsilon)_{i,A}$: Where i is decomposition level and (ϵ) denotes the detail sub-bands such as horizontal, vertical or diagonal detail. We carried the decomposition up to level 3.

3. Thresholding: The minimum and maximum value of coefficients of each detail sub-band at each level are determined by using the thresholding method, which preserved all low level informations less than a threshold. All low level pixels at each level provide the general information of image with the highest effective details.

4. Enhanced directional smoothing is applied at each detail sub band at each level $S(\epsilon)_{i,A}$ to protect the edges, based on the statistical relationship between the central pixel and its surrounding pixels.

5. Reconstruction is performed by using inverse undecimated wavelet transformation.

In the next phase, the multi-layer prediction network is made by training multiple independent networks. This multiple layer with various scales produce better results by combining the information of each side-output. In following, we denote the training set $S = (X_n, Y_n), n = 1, , N. X_n$ is initial provided image by UDWT and $Y_n = y_j^n, j = 1, , |X_n|, y_j^n 0, 1$, the predicted labels or the corresponding ground truth binary boundary map for image X_n. All standard network layer parameters is denoted as W, and for M side-output layers associated with a classifier, corresponding weights are denoted as $w = (w^{(1)}, ..., w^{(M)})$. The loss function of HED [16] is expressed as:

$$L_{side}(W, w) = \sum_{m=1}^{M} \alpha_m l^m(W, w^m) \tag{3}$$

Where l^m are the side-layer losses on the side output of the layer of m. The loss function is computed over all pixels in a training input image X_n and target or edge map Y_n. As a matter of fact, 90% of the ground truth is non-edge and the distribution of edge and non-edge pixels is extremely biased, The class-balanced cross-entropy loss function is used to make a cost-sensitive loss function for biased sampling:

$$l^m(W, w^m) = -\beta \sum_{j \in Y+} logP(y_j = 1 \mid X; W, w^m)$$
$$-(1-\beta) \sum_{j \in Y-} logP(y_j = 0 \mid X; W, w^m) \tag{4}$$
$$= \sum_{jY} w(y_j)S(y_j, s_j^m)$$

Where $Y-$ and $Y+$ denote the edge and non-edge ground truth label sets, respectively. Sigmoid function operation is used to calculate the equation $Pr(y_j = 1 \mid X; W, w^m)$ on the inner product $s_j^m = w^m, f_j$ between the side layer parameters and the feature f_j at position j, $P(y_j = 1 \mid X; W, w^m) = \sigma(s_j^m)$. Side-output predictions by using the weighted-fusion are added to the network and simultaneously learned the fusion weight during training. So, loss function becomes:
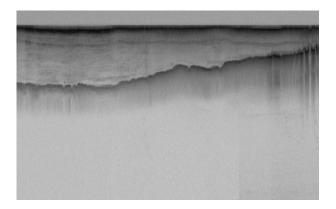
$$L_{fuse}(W, w, h) = Dist(Y, Y_f) \tag{5}$$

Fig. 2. Radar Image.

Where $Y_f use \sigma(\sum_{m=1}^{M} h_m A_s^m)$ and $h = (h_1, ..., h_M)$ is the fusion weight. Dist (Y, Y_f) is distance between the fused prediction and the ground truth label map. The overall objective function is written as follows:

$$L_{Final}(W, w, h) = L_{fuse}(W, w) + L_{fuse}(W, w, h) \quad (6)$$

It is optimized using common Stochastic Gradient Descent (SGD) training with momentum. The final unified output can be obtained by aggregation the generated edge maps from each side output and the weighed fusion layer:

$$Y_{Final} = Average(Y_{fuse}, Y_{side}^1, ..., Y_{side}^M) \quad (7)$$

3. EXPERIMENTAL RESULTS

In this work, we have used the radar images provided by NASA Operation IceBridge Mission from year 2009 for testing and 2010-2016 for training the network. In the first experiment, we used the pre-trained HED network with BSDS500 [20] which produced the F-measure = 0.73. In the next experiment, we trained the network with the ice images (2010-2016), which as expected the results reached a higher accuracy of boundary detection (f-measure = 0.751). Our deep hybrid undecimated wavelet network by training the network with ice data set from 2010 to 2016 provide the highest performance (0.771). We also compared this technique with two traditional techniques, canny and multiscale gradient magnitude (MSGM) technique [5]. The results are summarized in table 1.

3.1. Training With NASA Operation IceBridge Mission dataset

The hyper-parameters used in this implementation include: mini-batch size 10, learning rate $(1e - 6)$, loss-weight α_m for each side-output layer 1, momentum 0.9 of the fusion layer weights $1/5$, weight decay 0.0002, number of training iterations 10,000; divided learning rate by 10 after 5,000. To evaluate this algorithm, 820 images were used for training and
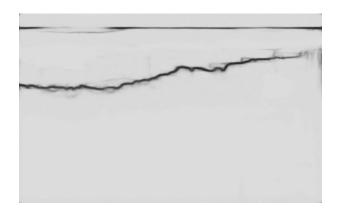

Fig. 3. The result of ice surface and bottom boundary detection

Table 1. The results of boundary detection techniques

Techniques	Precision	Recall	F-measure
Canny[2]	0.741	0.721	0.727
MSGM[5]	0.739	0.702	0.721
HED[16]	0.742	0.717	0.730
HED-ICE	0.782	0.722	0.751
Deep Hybrid net	**0.801**	**0.742**	**0.771**

100 images for testing. Ground-truth imgaes have been prepared by manualy labeling the images by human. The input and output images are shown in Figure 2 and Figure 3 .

3.2. Assessment

To evaluate the performance of our technique we calculated precision, recall, and F-measure on our testing dataset.*Precision* is the fraction of detections that are true positives rather than false positives, and *recall* is the fraction of true positives that are detected rather than missed. *F-measure* is the weighted harmonic mean of precision and recall.The balanced F-measure ($\beta = 1$) is used.

The performance of our techniques (Deep hybrid net) in comparison with Canny[2], MSGM[5], HED[16], pretrained with BSDS500 dataset (HED), and HED trained on Ice RADAR dataset (HED-ICE) is listed in table 1. Our deep hybrid network achieved the highest F-measure accuracy (0.771).

4. CONCLUSIONS

Here we presented a deep hybrid wavelet network for detecting ice surface and bottom boundaries from radar images. We reached the F-measure of 0.77 on the NASA Operation IceBridge Mission dataset. Our experimental results in comparison to the state-of-the-art techniques showed the efficiencyy of our technique.

6. REFERENCES

[1] Josef Kittler, "On the accuracy of the sobel edge detector," *Image and Vision Computing*, vol. 1, no. 1, pp. 37–42, 1983.

[2] John Canny, "A computational approach to edge detection," *IEEE Transactions on pattern analysis and machine intelligence*, , no. 6, pp. 679–698, 1986.

[3] David Marr and Ellen Hildreth, "Theory of edge detection," *Proceedings of the Royal Society of London B: Biological Sciences*, vol. 207, no. 1167, pp. 187–217, 1980.

[4] Piotr Dollar, Zhuowen Tu, and Serge Belongie, "Supervised learning of edges and object boundaries," in *Computer Vision and Pattern Recognition, 2006 IEEE Computer Society Conference on*. IEEE, 2006, vol. 2, pp. 1964–1971.

[5] Xiaofeng Ren, "Multi-scale improves boundary detection in natural images," *Computer Vision–ECCV 2008*, pp. 533–545, 2008.

[6] Piotr Dollár and C Lawrence Zitnick, "Fast edge detection using structured forests," *IEEE transactions on pattern analysis and machine intelligence*, vol. 37, no. 8, pp. 1558–1570, 2015.

[7] Adamo Ferro and Lorenzo Bruzzone, "Analysis of radar sounder signals for the automatic detection and characterization of subsurface features," *IEEE Transactions on Geoscience and Remote Sensing*, vol. 50, no. 11, pp. 4333–4348, 2012.

[8] Christopher M Gifford, Gladys Finyom, Michael Jefferson, MyAsia Reid, Eric L Akers, and Arvin Agah, "Automated polar ice thickness estimation from radar imagery," *IEEE Transactions on Image Processing*, vol. 19, no. 9, pp. 2456–2469, 2010.

[9] Greg J Freeman, Alan C Bovik, and John W Holt, "Automated detection of near surface martian ice layers in orbital radar data," in *Image Analysis & Interpretation (SSIAI), 2010 IEEE Southwest Symposium on*. IEEE, 2010, pp. 117–120.

[10] Maryam Rahnemoonfar, Geoffrey Charles Fox, Masoud Yari, and John Paden, "Automatic ice surface and bottom boundaries estimation in radar imagery based on level-set approach," *IEEE Transactions on Geoscience and Remote Sensing*, 2017.

[11] David J Crandall, Geoffrey C Fox, and John D Paden, "Layer-finding in radar echograms using probabilistic graphical models," in *Pattern Recognition (ICPR), 2012 21st International Conference on*. IEEE, 2012, pp. 1530–1533.

[12] Yaroslav Ganin and Victor Lempitsky, "Nˆ 4-fields: Neural network nearest neighbor fields for image transforms," in *Asian Conference on Computer Vision*. Springer, 2014, pp. 536–551.

[13] Wei Shen, Xinggang Wang, Yan Wang, Xiang Bai, and Zhijiang Zhang, "Deepcontour: A deep convolutional feature learned by positive-sharing loss for contour detection," in *Proceedings of the IEEE Conference on Computer Vision and Pattern Recognition*, 2015, pp. 3982–3991.

[14] Gedas Bertasius, Jianbo Shi, and Lorenzo Torresani, "Deepedge: A multi-scale bifurcated deep network for top-down contour detection," in *Proceedings of the IEEE Conference on Computer Vision and Pattern Recognition*, 2015, pp. 4380–4389.

[15] Jyh-Jing Hwang and Tyng-Luh Liu, "Pixel-wise deep learning for contour detection," *arXiv preprint arXiv:1504.01989*, 2015.

[16] Saining Xie and Zhuowen Tu, "Holistically-nested edge detection," in *Proceedings of the IEEE international conference on computer vision*, 2015, pp. 1395–1403.

[17] Fabrizio Argenti, Alessandro Lapini, Tiziano Bianchi, and Luciano Alparone, "A tutorial on speckle reduction in synthetic aperture radar images," *IEEE Geoscience and remote sensing magazine*, vol. 1, no. 3, pp. 6–35, 2013.

[18] Mark J Shensa, "The discrete wavelet transform: wedding the a trous and mallat algorithms," *IEEE Transactions on signal processing*, vol. 40, no. 10, pp. 2464–2482, 1992.

[19] Ronald W Schafer, "What is a savitzky-golay filter?[lecture notes]," *IEEE Signal processing magazine*, vol. 28, no. 4, pp. 111–117, 2011.

[20] David Martin and Charless Fowlkes, "The berkeley segmentation database and benchmark," *Computer Science Department, Berkeley University. http://www. eecs. berkeley. edu/Research/Projects/CS/vision/bsds*, 2001.